

# Automated design of pneumatic soft grippers through design-dependent multi-material topology optimization

Josh Pinski<sup>1</sup>, Prabhat Kumar<sup>2</sup>, David Howard<sup>1</sup>, and Matthijs Langelaar<sup>3</sup>

**Abstract**—In recent years, soft robotic grasping has rapidly spread through the academic robotics community and pushed into industrial applications. At the same time, multimaterial 3D printing has become widely available, enabling monolithic manufacture of devices containing rigid and elastic section. We propose a novel design technique which leverages both of these technologies and is able to automatically design bespoke soft robotic grippers for fruit-picking and similar applications. We demonstrate the novel topology optimisation formulation which generates multi-material soft grippers and is able to solve both the internal and external pressure boundaries, and investigate methods to produce air-tight designs. Compared to existing methods, it vastly expands the searchable design space whilst increasing simulation accuracy.

## I. INTRODUCTION

Soft robotic grasping has emerged as an safe and effective means for grasping fragile, flexible and fluctuating objects. Their inherent deformability enables them to conform to fit the objects' shape and distribute gripping force, hence gently grasping even soft objects.

These soft grippers are often inspired by human hands, which are seen as the gold standard in soft and dexterous grasping. However, there is an increasing trend towards non-anthropomorphic designs, which enable diverse grasping strategies and require controllable fewer degrees of freedom (DOFs) [1]. Several mechanisms have been investigated for their actuation including pneumatic [2], tendon-driven [3], and granular (vacuum) jamming [4], [5].

Despite the diversity of grasping and actuation paradigms available in the literature, most existing grippers are designed by hand. They draw on human experience and biomimicry to navigate the complexity of designing deformable devices to generate high-quality designs [6]. The resulting designs are normally generic, emphasizing universal approaches rather than bespoke designs [4]. However, real world applications frequently require designs which are tailored to the specifics of their task. Clearly a fruit picking robot requires a different end effector to an assembly line robot or a human assistance robot, and an apple-picking end-effector has different requirements to a strawberry picker. Despite this obvious

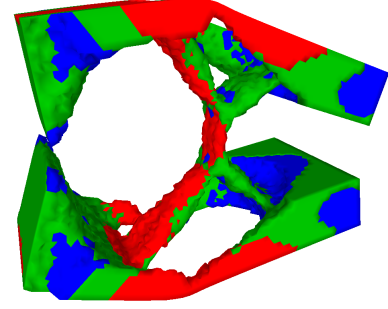


Fig. 1. 3 Material optimised soft-gripper under 50kPa pressure (5x deformation scale). Pressure is applied to the two faces on the left, causing the jaws to close on the right. Material stiffnesses are: Red - 100MPa, Green - 10MPa, Blue - 1MPa

need to produce bespoke soft end effectors, exiting automated design tools are limited and underexplored. Methods including simulated and in-material evolution have recently proven successful in designing granular jamming grippers [7], [8].

In contrast, Topology optimization (TO) is a general purpose design tool, suitable to numerous actuation techniques and physical domains [9]. It distributes material inside a meshed (or pixelized/voxelized) space to identify the topology with the best performance, and has designed both pneumatic and tendon-driven soft grippers. [10], [6], [11]. However, the methods presented in these works require significant assumptions about the design space and actuation, limiting both the accuracy of the simulation and the range of realisable designs.

### A. Topology Optimisation of Soft Grippers

The current state-of-the-art in topology optimised soft grippers broadly falls into two categories:

- 1) Externally actuated grippers [12], [10]. These use an exogenous displacement to drive their grasping behaviour, that is an externally routed cable or moving surface.
- 2) Pressure actuated soft fingers without design dependency [13], [14], [15]. These specify a pressure distribution on a fixed surface, which must be prespecified does not form part of the optimisation problem formulation.

In both of these cases, the actuation source is prespecified and does not form part of the optimisation problem. Whilst convenient, these assumptions do not reflect best-practice design methods which use complex pneumatic chambers

<sup>1</sup>Robotics and Autonomous Systems Group, CSIRO Data61, Brisbane, Australia josh.pinski@csiro.au, david.howard@csiro.au

<sup>2</sup>Department of Mechanical and Aerospace Engineering, Indian Institute of Technology Hyderabad, 502285 Telangana, India pkumar@mae.iith.ac.in

<sup>3</sup>Department of Precision and Microsystems Engineering, TU Delft, Delft, Netherlands m.langelaar@tudelft.nl

The authors thank Prof. Krister Svanberg for providing MATLAB codes of the MMA optimizer.

and internal cable routing. To capture these features, the loading point (magnitude, direction and location) should be free to move with each iteration of the topology optimisation solver. This design-dependency problem increases the solver complexity and requires auxiliary physics equations to solve and additional constraints to enforce physical limits. A small number of topology optimised soft grippers have investigated design-dependent pressure optimisation, but their coarse physics approximations result in unrealisable designs, with disconnected pressurised regions [16], [17].

Whilst the above methods have been demonstrated only single-material optimisation, improvements in 3D printing technology, enable the monolithic manufacture of arbitrarily complex multi-material soft robots. By using two or more materials, it is possible to strike a trade-off between the flexibility and strength of the material, and increase the overall strength of the device without compromising on its workspace. For a detailed review of soft robotic topology optimisation see [6], [18].

To the best of the authors' knowledge, there is currently no method for creating multi-material pneumatically activated soft robots using topology optimization.

### B. Pressure-Loaded Topology Optimisation

Pressure-loaded topology optimisation is a problem which extends beyond soft robotics. It has applications in the design of pneumatically and hydraulically loaded structures like pressure vessels, dams, pumps and ships. In these problems, the fluid-solid boundary and hence the loading must move during the optimisation. In density-based topology optimisation, mesh elements are allowed to occupy a continuum between solid and void [9]. Hence, the problem is commonly approached either by attempting to explicitly identify a fluid-solid boundary, or using a mixed fluid-solid formulation [19], [20]. Whilst the mixed-method overcomes the challenges of identifying a unique boundary, it introduces an additional material phase (solid/fluid/void rather than solid/void) whose volume must be specified prior to optimisation. The current state of the art method treats the continuous density material as a porous media, and uses the Darcy method to estimate fluid penetration as a function of density [20], [11].

Whilst the Darcy method is state of the art for pneumatically actuated mechanisms, there is no guarantee that the design will be airtight. In both the Darcy method and other pneumatic compliant mechanism formulations, the optimisation frequently results in undesirable holes in the structure. As there is no constraint placed on flow-rate, these reduce stiffness and hence increase calculated output displacement. Whilst this can be addressed using a material filtering scheme, which forces a solid layer between the high and low pressure regions [21], such a scheme is heavily dependent on the optimisers initial conditions, and prevents the formation of beneficial internal cavities.

### C. Contributions

In this work, we present a novel method to design 3D multi-material pressure-actuated soft grippers using topology

optimization. The method builds on our previous work into pressure-loaded topology optimization using Darcy's law [20], [11] and the extended solid-isotropic material with penalisation (SIMP) material model for the multi-material modeling [22]. An example of a soft gripper designed using this method is shown in Figure 1, it uses three materials with stiffnesses of 1 MPa, 10 MPa and 100 MPa. Using the multimaterial Darcy formulation, the solver converges to a soft gripper which clamps together using several compliant hinges.

The main contributions of this work are:

- 1) The first presentation of a multi-material topology optimisation formulation for pneumatic soft robots
- 2) The development and investigation two new formulations to generate sealed pneumatic actuators, based on pressure regions and an energy penalty, respectively.
- 3) The design of several new multimaterial pressure-actuated soft grippers.

Whilst we focus on the application of this methodology to soft robotic grasping, it is generalisable to other pneumatic compliant mechanism and soft robots.

## II. TOPOLOGY OPTIMISATION FORMULATION

In this work, we use the density based SIMP method for topology optimisation. The goal of topology optimisation is to find a discrete material layout where each region contains a unique material or is left void. To simplify the problem, SIMP allows the design variable  $\rho$  to occupy a continuum from 0 to 1, and a penalty  $p$  applied to drive the results towards a binary solution. For a single material problem this is done using the SIMP interpolation law:

$$E_i = (1 - \bar{\rho}^p)E_{\min} + \bar{\rho}^p E_1 \quad (1)$$

where  $E_{\min}$  is a small, non-zero constant used to prevent singularities in material voids and  $E_1$  is the elastic modulus of the material used.

### A. Multimaterial Modeling

To model multiple materials for the gripper mechanisms, we apply the extended SIMP interpolation technique [9]. In this formulation, one design variable is assigned to each material. For example, in the two-material case, the scheme with the modified SIMP formulation can be written as:

$$E_i = (1 - \bar{\rho}_{i1}^p)E_{\min} + \bar{\rho}_{i1}^p((1 - \bar{\rho}_{i2}^p)E_1 + \bar{\rho}_{i2}^p E_2), \quad (2)$$

where  $E_1$  and  $E_2$  are moduli of material 1 and material 2, respectively.  $\bar{\rho}_i$  denotes the physical variable corresponding to design variable  $\rho_i$ , and the SIMP parameter  $p$  is set to 3.  $\{\bar{\rho}_{i1} = 1, \bar{\rho}_{i2} = 1\}$  gives the second material, whereas  $\{\bar{\rho}_{i1} = 1, \bar{\rho}_{i2} = 0\}$  provides the first material. Thus,  $\bar{\rho}_{i1}$  is called the topology variable, i.e., it decides the topology of the evolving design, whereas  $\bar{\rho}_{i2}$  decides the candidate material. Similarly the three-material case can be described by:

$$E_i = (1 - \bar{\rho}_{i1}^p)E_{\min} + \bar{\rho}_{i1}^p[[(1 - \bar{\rho}_{i2}^p)E_1 + \bar{\rho}_{i2}^p((1 - \bar{\rho}_{i3}^p)E_2 + \bar{\rho}_{i3}^p E_3)]], \quad (3)$$

where  $E_3$  is the modulus of material 3. Using three materials,  $\{\bar{\rho}_{i1} = 1, \bar{\rho}_{i2} = 0, \bar{\rho}_{i3} = 0\}$ ,  $\{\bar{\rho}_{i1} = 1, \bar{\rho}_{i2} = 1, \bar{\rho}_{i3} = 0\}$  and  $\{\bar{\rho}_{i1} = 1, \bar{\rho}_{i2} = 1, \bar{\rho}_{i3} = 1\}$  give respectively material 1, material 2 and material 3.

To remove non-physical checkerboard patterns and intermediate (i.e non-binary) densities from the final design, we use density and hyperbolic projection filters as in [9], [23].

### B. Pressure load modeling

This section describes the pressure load modeling scheme using the Darcy law with the conceptualized drainage term. The method developed here for pneumatic soft robotic optimisations builds on our previous work into the Darcy method, a detailed description of which can be found in [20], [11]. It conceptualises the continuous design variable  $\bar{\rho}$  as a porous medium, and uses Darcy's law to calculate pressure losses. In it, the flux  $\mathbf{q}$  (volumetric fluid flow rate across a unit area) is defined by the flow coefficient  $K(\bar{\rho}_{i1})$  and the pressure difference  $\nabla p$  as:

$$\mathbf{q} = -\frac{\kappa}{\mu} \nabla p = -K(\bar{\rho}_{i1}) \nabla p \quad (4)$$

As the topology of the multimaterial structure (whether there is a material or void) is determined by  $\bar{\rho}_{i1}$ , the flux solely depends on  $\bar{\rho}_{i1}$ , regardless of the number of materials. Hence, the flow coefficient of element  $i$  is calculated as

$$K(\bar{\rho}_i) = K_v \left( 1 - \left( 1 - \frac{K_s}{K_v} \right) \mathcal{H}(\bar{\rho}_{i1}, \beta_\kappa, \eta_\kappa) \right), \quad (5)$$

where

$$\mathcal{H}(\bar{\rho}_{i1}, \beta_\kappa, \eta_\kappa) = \frac{\tanh(\beta_\kappa \eta_\kappa) + \tanh(\beta_\kappa (\bar{\rho}_{i1} - \eta_\kappa))}{\tanh(\beta_\kappa \eta_\kappa) + \tanh(\beta_\kappa (1 - \eta_\kappa))}, \quad (6)$$

$K_s$  and  $K_v$  are flow coefficients of solid and void phases, respectively, and  $\eta_\kappa$  and  $\beta_\kappa$  shape the distribution of  $K(\bar{\rho}_i)$ .

Finally, a drainage term,  $Q_{\text{drain}}$ , is added. It helps achieve the natural pressure field variation by draining pressure from internal cavities:

$$Q_{\text{drain}} = -D_s \mathcal{H}(\bar{\rho}_{i1}, \beta_d, \eta_d) (\bar{\rho}_e) (p - p_{\text{stm}}) \quad (7)$$

where  $D_s$  is drainage coefficient and  $p_{\text{atm}}$  is the atmospheric pressure. The net flow of the system is given by the equilibrium equation:

$$\nabla \cdot \mathbf{q} - Q_{\text{drain}} = 0. \quad (8)$$

. Which is solved using the finite element method to find the equilibrium pressure distribution and transform the pressure distribution  $\mathbf{p}$ , to a global force  $\mathbf{F}$  to solve the mechanical equilibrium equation:

$$\mathbf{K}\mathbf{u} = \mathbf{F} = -\mathbf{T}\mathbf{p} \quad (9)$$

where  $\mathbf{u}$  and  $\mathbf{K}$  are the global displacement vector and stiffness matrix, and  $\mathbf{T}$  transforms elemental pressures to nodal forces. By using two physical equation to solve for the equilibrium pressure and displacement, the formulation determines the pressure boundary at each iteration.

### C. Problem formulation

The final optimisation problem is formulated using:

$$\left. \begin{array}{l} \min_{\rho} \quad -s \frac{u_{\text{out}}}{(SE)^{1/n}} \\ \text{such that:} \quad \mathbf{A}\mathbf{p} = \mathbf{0} \\ \quad \mathbf{K}\mathbf{u} = \mathbf{F} = -\mathbf{T}\mathbf{p} \\ \quad \sum_{i=1}^{\text{nel}} v_i \bar{\rho}_{i1} \leq (v_{f1} + v_{f2} + v_{f3}) \sum_{i=1}^{\text{nel}} v_i \\ \quad \sum_{i=1}^{\text{nel}} v_i \bar{\rho}_{i2} \leq v_{f2} \sum_{i=1}^{\text{nel}} v_i \\ \quad \sum_{i=1}^{\text{nel}} v_i \bar{\rho}_{i3} \leq v_{f3} \sum_{i=1}^{\text{nel}} v_i \\ \quad 0 \leq \bar{\rho} \leq 1 \end{array} \right\}, \quad (10)$$

Data:  $v_{f1}, v_{f2}, v_{f3}, E_1, E_2, E_3, p$

where  $u_{\text{out}}$  and  $SE$  indicate output displacement and strain energy, respectively.  $s$  is the consistent scaling parameter.  $\mathbf{A}$  is the global flow matrix, which is found by assembling (8). We use three linear volume constraints using the definitions  $\bar{\rho}_{i1}$ ,  $\bar{\rho}_{i2}$  and  $\bar{\rho}_{i3}$  described above. The first constraint controls the total amount of the solid state, whereas the second and third give the material amount of phase 2 and phase 3.  $v_{f1}k$ ,  $v_{f2}$  and  $v_{f3}$  denote the volume fraction for material 1, material 2 and material 3, respectively.

The cost function is selected to balance the dual requirements of maximising the deformation of the gripper, and maintaining a design which is stiff enough to grasp and hold objects. Here  $n = 8$  is used to place a soft penalty on the design's stiffness. In this work  $v_{f1} = 0.3$ ,  $v_{f2} = 0.2$ , and  $v_{f3} = 0.2$  unless otherwise stated, and the input pressure is 50 kPa and the materials are given stiffnesses  $E_1 = 1$  MPa,  $E_2 = 10$  MPa, and  $E_3 = 100$  MPa

## III. SOFT GRIPPERS DESIGN

To demonstrate the method and motivate the need for airtightness, this section investigates the design of pressure actuated grippers using the multimaterial Darcy formulation. The design space of the grippers is presented in Figure 2(a). Pressure is applied from the left face, with the output direction shown on the right. To simplify the design space and reduce computation time, 2 planes of symmetry are used, reducing the size of the workspace.

The resulting design is illustrated in , showing the undeformed and deformed configuration. In it, a solid face is formed on the left side, which absorbs the pressure. The internal strains are then transferred to the output face via a series of compliant hinges, one in the centre of the gripper, and four on the outer edges. To give the design stiffness, thin sections of the stiffest material  $E_3$  are used in each of the hinges, and joined by the softer materials  $E_1$  and  $E_2$ . Whilst quite elegant, the design illustrates two issues with existing pressure optimisation methods. The first is that the optimiser frequently falls into a local minima in which the pressurised

fluid is not allowed to penetrate deeply into the structure, preventing the formation of more complex, higher performing designs. The second is that without careful consideration of the design space, the optimiser generates holes in the final design which spuriously increases performance by reducing stiffness in undesired locations. In this case, resealing the device is fairly trivial, but in more complex designs, doing so adversely affects performance. Hence, design methods are needed which drive closed designs.

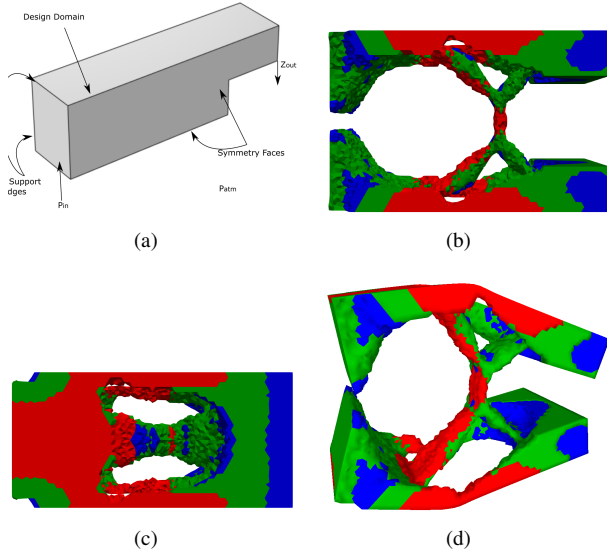


Fig. 2. 3 Material optimised soft-gripper with stiffnesses: Red - 100MPa, Green - 10MPa, Blue - 1MPa, (a) Design domain (b) Undeformed Side-view (c) Undeformed top-view (d) Deformed (5x deformation scale)

#### IV. AIRTIGHT DESIGN

To generate closed designs, we investigate and compare three methods, and apply them to soft finger design. In soft fingers, the pressure load is often applied via a central channel in the design space. Whilst this forces pressure deeper into the design and enhances performance, it also increases its susceptibility to hole generation. Viewed from the perspective of the optimisation problem, sealed chambers increase the stiffness of the device and restrict output motion. We propose two new methods for generating sealed designs:

- 1) A heuristic approach, which adds material to the final design along the median pressure contour.
- 2) A penalty approach, which adds an energy term to the cost function and drives the optimisation to reduce pressure loss.

The first approach leverages the advantages of the Darcy method, which calculates the internal pressure distribution between the inlet and outlet points. Where a face is unsealed, there will be a smooth gradient of pressure flowing from the inlet to outlet. However, closed regions have a sharper pressure boundary. Hence by adding material along the line  $0.5 * (p_{in} - p_{out})$  we close open regions without significantly impacting regions which already have material.

The second approach is more rigorous, but remains susceptible to local minima. Using the equilibrium flow from the Darcy equation, we are able to calculate the energy transferred from inlet to outlet. In a closed system there would be no flow, hence no energy transferred. However, using the Darcy method, a small flow will always arise. We use this energy value as a penalty term in the cost function, such that we seek to minimise:

$$\min_{\rho} \left\{ -s \frac{u_{out}}{E_t (SE)^{1/n}} \right\} \quad (11)$$

where  $E_t$  is the total energy loss.

#### V. AIRTIGHT SOFT FINGERS

The design space of the soft fingers is presented in 3(a). It is fixed around the edges on the left side and pressure enters via a central cavity, a single symmetry face is used to reduce the problem size. The aim is to maximise the bending on the right side.

##### A. Heuristic Skin

An example of the design of the bending soft finger is shown in Figure 3. Without any closure method, the material is distributed roughly from stiffest to softest, with the stiffest material placed around the fixed side. Bending is increased by placing holes at the top and sides of the structure. However, a closed structure is easily regenerated using the heuristic methods

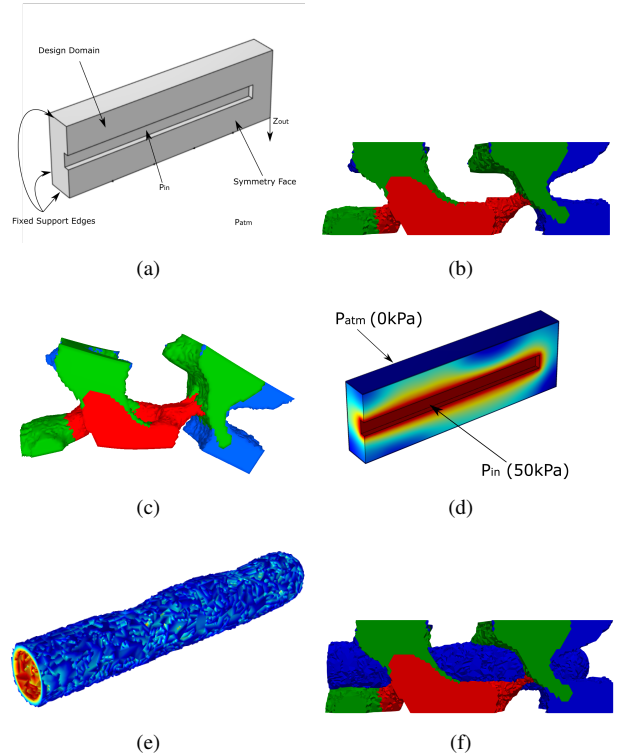


Fig. 3. 3 Material optimised soft-finger with stiffnesses: Red - 100MPa, Green - 10MPa, Blue - 1MPa, (a) Design domain (b) Undeformed (c) Deformed (5x deformation scale) (d) Optimised Pressure Distribution (Undeformed) (e) Implied pressure boundary (f) Complete design with sealed chamber

### B. With Skin

The surface can also be inserted as part of the optimisation problem by creating a non-design domain on the boundary of the optimisation region and assigning it to have stiffness  $E_1$ . This guarantees air cannot leak, but will produce suboptimal solutions as the external boundary must bend and expand to generate deformation. In contrast, pnueenets, a state of the art designs have sinusodal profiles which localise bending. This result is illustrated in Figure 4.

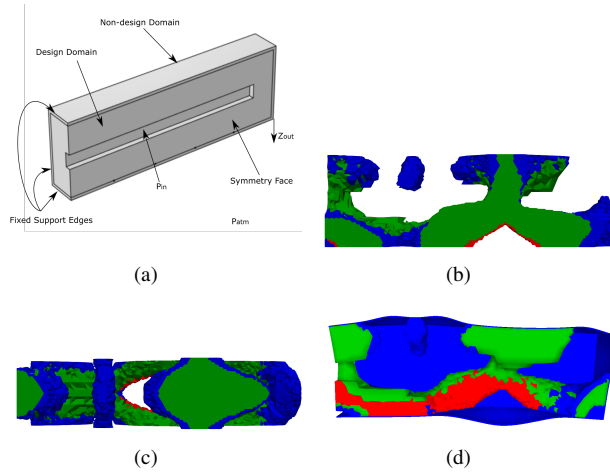


Fig. 4. 3 Material optimised soft-finger with casing - stiffnesses: Red - 100MPa, Green - 10MPa, Blue - 1MPa, (a) Design domain (b) Undeformed Side-view (casing not shown) (c) Undeformed top-view (casing not shown) (d) Deformed half model, showing casing (5x deformation scale)

### C. Energy Penalty

Finally, the same design is presented using the energy penalty method. Here, the optimiser has reduced the overall amount of air leakage by using the low stiffness material  $E_1$  to close sections of the chamber which contribute least to bending. The result is not a totally closed design, but one where the open areas have been greatly reduced. This uses the same design space as the heuristic skin. The efficacy of

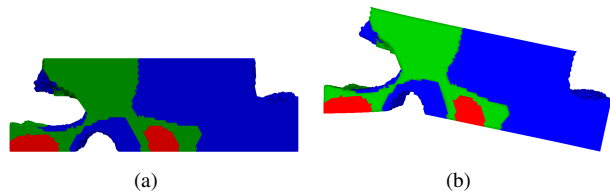


Fig. 5. Energy Penalised soft-gripper (a) Undeformed (b) Deformed (5x deformation scale)

this of this penalty can be increased by allowing more or lower stiffness materials to be included as is illustrated in 6. When using  $V_{f1} = 0.2$ , there is insufficient material to meaningfully close the design, but at  $V_{f1} = 0.4$  an almost sealed chamber emerges with only a small opening around the fixed side. Whilst the remaining opening is not ideal, it is relatively simple to close in postprocessing

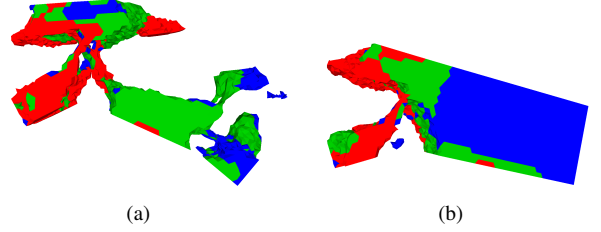


Fig. 6. Energy Penalised soft-gripper with (a)  $V_{f1} = 0.2$  (b)  $V_{f1} = 0.4$

### D. Numerical Comparison

We compare the two proposed closure methods by calculating their output displacement, strain energy, mechanical work done, and energy loss across 9 different output stiffnesses (springs placed at the output face) from  $0.1N/m$  to  $1000N/m$ . The results are presented in Figure 7. Unsurprisingly, the unconstrained (no skin) optimisation has by far the highest bending, strain energy, work done and energy loss. Ignoring the energy loss, the design performs extremely well. In contrast, the closed design space performs extremely poorly, and is a poor choice of closure method. Of the two methods discussed in this work, the heuristic gives the best performance, with a relatively large output displacement and low strain energy and energy loss. Whilst the energy penalty shows promise, it is impeded by the gradient based solve, and minimum length scales of topology optimisation, which prevent the formation of thin skins.

## VI. DISCUSSION AND CONCLUSION

Guaranteeing closure remains a problem in this method, and something which has not been solved in existing research. We discussed two new methods for generated closed or near closed soft robots. Of the two, the heuristic approach outperforms the optimisation method. However the latter approach is worthy of further investigation. In addition, this work presented a multi-material method for pneumatic topology optimisation and presented several new soft gripper designs. By tweaking the design space and choosing different output points and stiffnesses, the method is able to generate bespoke grippers for specific applications such as fruit harvesting or human interaction. We aim to integrate it into soft robotic pick and place systems and experimentally verify its performance in the future.

## REFERENCES

- [1] Y. Hao and Y. Visell, "Beyond Soft Hands: Efficient Grasping With Non-Anthropomorphic Soft Grippers," *Frontiers in Robotics and AI*, vol. 8, no. July, pp. 1–8, 2021.
- [2] B. Mosadegh, P. Polygerinos, C. Keplinger, S. Wennstedt, R. F. Shepherd, U. Gupta, J. Shim, K. Bertoldi, C. J. Walsh, and G. M. Whitesides, "Pneumatic Networks for Soft Robotics that Actuate Rapidly," *Advanced Functional Materials* 24, vol. 24, no. 15, pp. 2163–2170, 2014.
- [3] C. Laschi, M. Cianchetti, B. Mazzolai, L. Margheri, M. Follador, and P. Dario, "Soft robot arm inspired by the octopus," *Advanced Robotics*, vol. 26, no. 7, pp. 709–727, 2012.
- [4] E. Brown, N. Rodenberg, J. Amend, A. Mozeika, E. Steltz, M. R. Zakin, H. Lipson, and H. M. Jaeger, "Universal robotic gripper based on the jamming of granular material," *Proceedings of the National Academy of Sciences of the United States of America*, vol. 107, no. 44, pp. 18809–18814, 2010, 1009.4444.

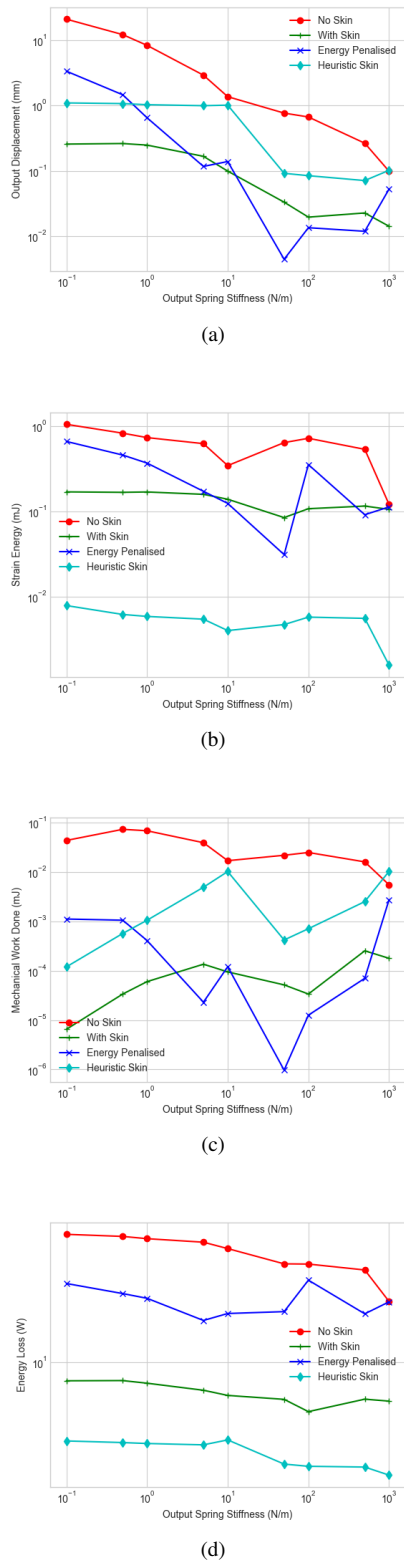


Fig. 7. Energy Penalised soft-gripper with  $V1 = 0.4$  (a) Displacement (b) Strain Energy (c) Mechanical work exerted on spring (d) Energy Loss

[5] G. D. Howard, J. Brett, J. O'Connor, J. Letchford, and G. W. Delaney, "One-Shot 3D-Printed Multimaterial Soft Robotic Jamming Grippers," *Soft Robotics*, vol. 00, no. 00, pp. 1–12, 2021.

[6] J. Pinski and D. Howard, "From Bioinspiration to Computer Generation: Developments in Autonomous Soft Robot Design," *Advanced Intelligent Systems*, vol. 4, no. 1, p. 2100086, 2022.

[7] D. Howard, J. O'Connor, J. Letchford, J. Brett, T. Joseph, S. Lin, D. Furby, and G. W. Delaney, "Getting a Grip: in Materio Evolution of Membrane Morphology for Soft Robotic Jamming Grippers," *2022 IEEE 5th International Conference on Soft Robotics, RoboSoft 2022*, pp. 531–538, 2022, 2111.01952.

[8] S. G. Fitzgerald, G. W. Delaney, D. Howard, and F. Maire, "Evolving soft robotic jamming grippers," *GECCO2021*, pp. 102–110, 2021.

[9] O. Sigmund and K. Maute, "Topology optimization approaches," *Structural and Multidisciplinary Optimization*, vol. 48, no. 6, pp. 1031–1055, 2013.

[10] F. Chen, W. Xu, H. Zhang, Y. Wang, J. Cao, M. Y. Wang, H. Ren, J. Zhu, and Y. Zhang, "Topology optimized design, fabrication, and characterization of a soft cable-driven gripper," *IEEE Robotics and Automation Letters*, vol. 3, no. 3, pp. 2463–2470, 2018.

[11] P. Kumar and M. Langelaar, "On topology optimization of design-dependent pressure-loaded three-dimensional structures and compliant mechanisms," *International Journal for Numerical Methods in Engineering*, vol. 122, no. 9, pp. 2205–2220, 2021.

[12] C. H. Liu, T. L. Chen, C. H. Chiu, M. C. Hsu, Y. Chen, T. Y. Pai, W. G. Peng, and Y. P. Chiang, "Optimal design of a soft robotic gripper for grasping unknown objects," *Soft Robotics*, vol. 5, no. 4, pp. 452–465, 2018.

[13] H. Zhang, A. S. Kumar, F. Chen, J. Y. Fuh, and M. Y. Wang, "Topology optimized multimaterial soft fingers for applications on grippers, rehabilitation, and artificial hands," *IEEE/ASME Transactions on Mechatronics*, vol. 24, no. 1, pp. 120–131, 2019.

[14] C. H. Liu, L. J. Chen, J. C. Chi, and J. Y. Wu, "Topology Optimization Design and Experiment of a Soft Pneumatic Bending Actuator for Grasping Applications," *IEEE Robotics and Automation Letters*, pp. 1–8, 2022.

[15] S. Chen, F. Chen, Z. Cao, Y. Wang, Y. Miao, G. Gu, and X. Zhu, "Topology Optimization of Skeleton-Reinforced Soft Pneumatic Actuators for Desired Motions," *IEEE/ASME Transactions on Mechatronics*, vol. 26, no. 4, pp. 1745–1753, 2021.

[16] Y. Chen, Z. Xia, and Q. Zhao, "Optimal Design of Soft Pneumatic Bending Actuators Subjected to Design-Dependent Pressure Loads," *IEEE/ASME Transactions on Mechatronics*, vol. 24, no. 6, pp. 2873–2884, 2019.

[17] B. Caasenbrood, A. Pogromsky, and H. Nijmeijer, "A Computational Design Framework for Pressure-driven Soft Robots through Nonlinear Topology Optimization," *2020 3rd IEEE International Conference on Soft Robotics, RoboSoft 2020*, no. July, pp. 633–638, 2020.

[18] F. Chen and M. Y. Wang, "Design Optimization of Soft Robots: A Review of the State of the Art," *IEEE Robotics and Automation Magazine*, no. December, pp. 27–43, 2020.

[19] O. Sigmund and P. M. Clausen, "Topology optimization using a mixed formulation: An alternative way to solve pressure load problems," *Computer Methods in Applied Mechanics and Engineering*, vol. 196, no. 13–16, pp. 1874–1889, 2007.

[20] P. Kumar, J. Frouws, and M. Langelaar, "Topology optimization of fluidic pressure-loaded structures and compliant mechanisms using the Darcy method," *Structural and Multidisciplinary Optimization*, vol. 61, pp. 1637–1655, 2020.

[21] E. M. de Souza and E. C. N. Silva, "Topology optimization applied to the design of actuators driven by pressure loads," *Structural and Multidisciplinary Optimization*, vol. 61, no. 5, pp. 1763–1786, 2020.

[22] O. Sigmund and S. Torquato, "Design of materials with extreme thermal expansion using a three-phase topology optimization method," *Journal of the Mechanics and Physics of Solids*, vol. 45, no. 6, pp. 1037–1067, 1997.

[23] T. E. Bruns and D. A. Tortorelli, "Topology optimization of non-linear elastic structures and compliant mechanisms," *Computer methods in applied mechanics and engineering*, vol. 190, no. 26–27, pp. 3443–3459, 2001.